Staphylococcus epidermidis surfactant peptides promote biofilm maturation and dissemination of biofilm-associated infection in mice

Rong Wang, Burhan A. Khan, Gordon Y. C. Cheung, Thanh-Huy L. Bach, Max Jameson-Lee, Kok-Fai Kong, Shu Y. Queck, and Michael Otto

Laboratory of Human Bacterial Pathogenesis, National Institute of Allergy and Infectious Diseases, NIH, Bethesda, Maryland, USA.

Biofilms are surface-attached agglomerations of microorganisms embedded in an extracellular matrix. Biofilm-associated infections are difficult to eradicate and represent a significant reservoir for disseminating and recurring serious infections. Infections involving biofilms frequently develop on indwelling medical devices in hospitalized patients, and *Staphylococcus epidermidis* is the leading cause of infection in this setting. However, the molecular determinants of biofilm dissemination are unknown. Here we have demonstrated that specific secreted, surfactant-like *S. epidermidis* peptides — the β subclass of phenol-soluble modulins (PSMs) — promote *S. epidermidis* biofilm structuring and detachment in vitro and dissemination from colonized catheters in a mouse model of device-related infection. Our study establishes in vivo significance of biofilm detachment mechanisms for the systemic spread of biofilm-associated infection and identifies the effectors of biofilm maturation and detachment in a premier biofilm-forming pathogen. Furthermore, by demonstrating that antibodies against PSMβ peptides inhibited bacterial spread from indwelling medical devices, we have provided proof of principle that interfering with biofilm detachment mechanisms may prevent dissemination of biofilm-associated infection.

Introduction

Surface-attached cellular agglomerations of microorganisms called biofilms are an important virulence determinant in bacteria (1), mainly because biofilm formation significantly increases resistance to antibiotics and host defenses (2). Many biofilm-associated infections occur in the hospital setting by contamination of indwelling medical devices from the epithelial flora of the patient or health care personnel. *Staphylococcus epidermidis*, a normal inhabitant of human skin, is the predominant causative agent of these infections (3). Importantly, bacterial dissemination from biofilm-infected catheters represents the most frequent source of severe *S. epidermidis* infections such as sepsis (4). Especially neonates often develop sepsis from *S. epidermidis* catheter infection, and *S. epidermidis* infection is a significant global source of morbidity and death, particularly in very low birth weight infants (5).

The formation of a biofilm begins with the attachment of bacteria to a surface and is followed by proliferation and maturation, which ultimately leads to the characteristic 3D biofilm structure with mushroom-shaped bacterial agglomerations surrounded by fluid-filled channels (6). Later, cells may detach from the biofilm in a process believed to be of crucial importance for the dissemination of a biofilm-associated infection. The molecular basis of biofilm maturation and detachment is poorly understood, but presumably involves mechanisms to disrupt cell-cell adhesion. In vitro evidence obtained in *Pseudomonas aeruginosa* and *Bacillus subtilis* indicates cell-cell disruption may be accomplished by surfactants (7–10), while enzymatic digestion of biofilm matrix molecules appears to promote biofilm detachment in *Actinobacillus actinomycetemcomitans* (11). These mechanisms are commonly under control of cell density ("quorum sensing") and are likely to ascertain a tightly regulated degree of biofilm expansion (12, 13). In staphylococci, the molecular effectors of cell-cell disruption during biofilm development are not known. Furthermore, whether biofilm detachment mechanisms contribute to the in vivo dissemination of biofilm-associated infection has not been investigated in any bacterium.

We and others have identified a family of short staphylococcal peptides, the phenol-soluble modulins (PSMs) (14, 15), which are strictly regulated by the quorum-sensing system *agr* (16–18) and whose amphiphilic α-helical structure suggests surfactant-like properties. This prompted us to analyze the role of PSMs in biofilm development. In the present study, we demonstrate that the β-type PSMs represent key effectors of *S. epidermidis* biofilm maturation and detachment. Furthermore, we show that these peptides facilitate the dissemination of biofilm-associated infection, providing evidence for in vivo significance of biofilm detachment.

Results

PSMβ peptides are the main PSM type produced in S. epidermidis biofilm culture. To investigate the role of PSMs in biofilms, we first determined production of PSM peptides in planktonic versus biofilm culture. We found that PSM production was overall lower in biofilm culture, while relative production of β-type PSMs was significantly increased (Figure 1). Of note, β-type PSMs were virtually the only PSM type produced in the biofilm mode of growth. We detected similar production patterns in all *S. epidermidis* strains in our collec-

Authorship note: Rong Wang, Burhan A. Khan, and Shu Y. Queck contributed equally to this work.

Conflict of interest: The authors have declared that no conflict of interest exists.

Citation for this article: *J Clin Invest.* 2011;121(1):238–248. doi:10.1172/JCI42520.

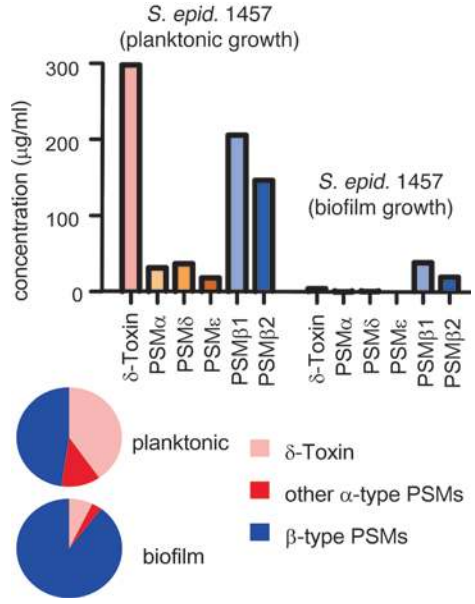

Figure 1
PSM production under biofilm and planktonic modes of growth. PSM production under planktonic (shaken 125 ml flasks containing 50 ml TSB/0.5% glucose, 18 hour growth, 37°C) or biofilm (24 hour static culture in microtiter plates, 37°C) modes of growth was assayed by RP-HPLC/ESI-MS. PSMs were determined in supernatants of planktonic or biofilm cultures after centrifugation. Absolute amounts are shown at the top, relative composition at the bottom. *S. epid.* 1457, *S. epidermidis* 1457.

tion, with the exception of 24 strains that completely lacked production of PSMs, including the *agr*-encoded δ-toxin. Thus, they are most likely naturally occurring mutants in the *agr* quorum–sensing system, whose deletion or lack of functionality leads to absence of PSM production (16–18). Of note, all those 24 strains were shown to contain *psm*β genes by analytical PCR (data not shown).

*The psm*β *locus forms a transcriptional unit.* β-type PSMs are distinguished from α-type PSMs and δ-toxin (~20–25 amino acids) by their larger size (~45 amino acids) and absence of cytolytic activity at physiological concentrations (18). As PSM production patterns suggested that especially the β-type PSMs may play a role in biofilm development, we first analyzed organization and transcription of the *psm*β genes (Figure 2A). The *psm*β operon is composed of 4 genes in strains *S. epidermidis* ATCC12228 and RP62A (19, 20), whose genome sequences are available, while the clinical isolate 1457 (21) used in our study has only 3 *psm*β genes. This is due to an exact duplication of the *psmβ1* gene in strains ATCC12228 and RP62A, while we determined by DNA sequencing that this duplication is missing from strain 1457. The remaining sequence of the *psm*β locus of strain 1457 was exactly the same as in ATCC12228. In the shotgun-sequenced strain M23864, the *psm*β operon appears to consist of 5 genes with slightly different peptide products. In keeping with the *psmβ1* gene duplication, strains RP62A and ATCC12228 secreted more PSMβ1 than PSMβ2, but combined production of the PSMβ peptides was not higher than in strain 1457 (data not shown). Furthermore, we never detected a peptide in culture filtrates of any *S. epidermidis* strain corresponding to the gene product of the *psmβ3* gene, indicating that the hypothetical PSMβ3 peptide is not secreted. To analyze whether the *psm*β genes form an operon, and thus are transcribed together, we performed Northern blot analysis (Figure 2B). We detected 1 predominant band, whose size corresponded exactly to the postulated size of a transcript comprising all 3 *psm*β genes of strain 1457, which therefore form an operon.

PSM peptides influence S. epidermidis biofilm formation in vitro. To investigate whether PSMβ peptides impact biofilm development, we first assayed in vitro biofilm formation with synthetic PSMβ peptides. The peptides were added to growing biofilm cultures of an *agr* mutant

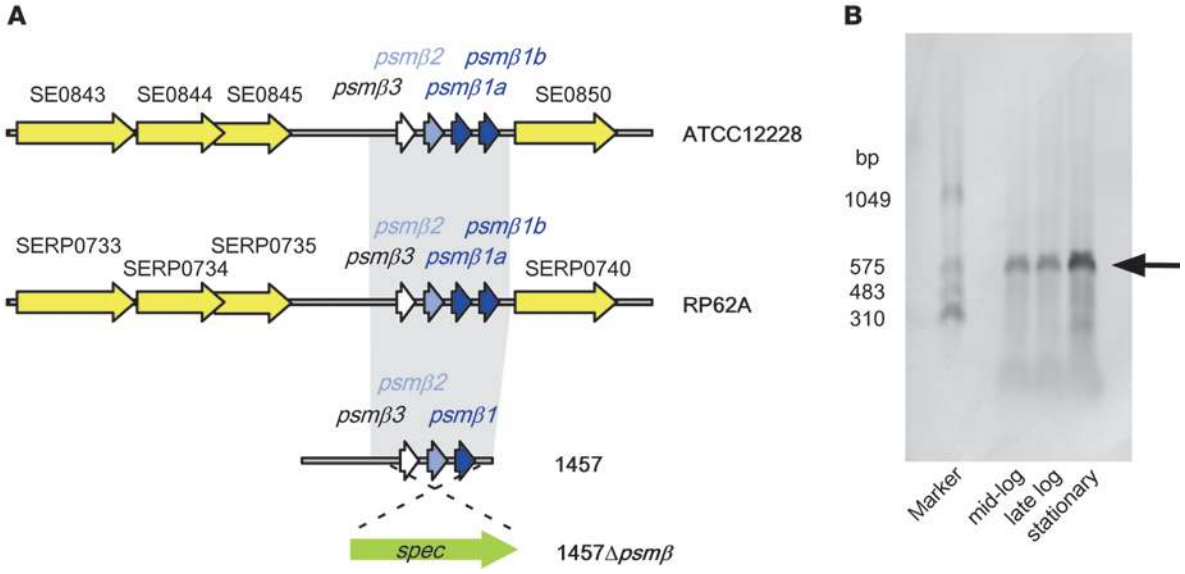

Figure 2
The *psm*β operon. (**A**) Organization of the *psm*β locus in genome-sequenced *S. epidermidis* strains and the 1457 strain used in this study. Construction of the *psm*β mutant allelic replacement strain is shown at the bottom. (**B**) Northern blot analysis of *S. epidermidis* 1457 RNA from different growth phases using a *psm*β probe. The *psm*β signal is marked by an arrow.

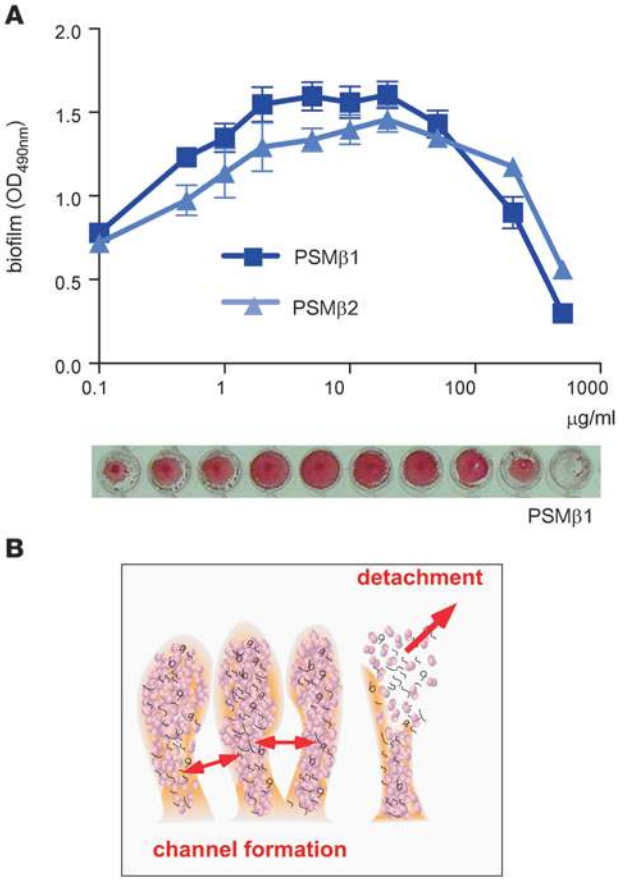

Figure 3

S. epidermidis in vitro biofilm formation under influence of PSMβ peptides. (**A**) Biofilm formation in microtiter plates (24 hours, 37°C). PSMβ peptides at different concentrations were added at the time of inoculation with *S. epidermidis agr* (devoid of PSMs). Biofilms were made visible using safranin staining (see example for PSMβ1 at the bottom), and biofilm formation was measured using an ELISA reader. Error bars depict mean ± SEM. (**B**) Schematic presentation of biofilm cell-cell disruptive processes leading to channel formation and detachment.

of strain 1457 (22), which owing to strict regulation of PSMs by *agr* (16–18), is devoid of PSM production. The PSMβ peptides promoted biofilm formation in a medium concentration range, while they inhibited biofilm formation at higher concentrations (Figure 3A). Of note, this phenotype is in accordance with a putative function of PSMβ peptides in cell-cell disruption on the molecular level (3, 23): at lower concentrations, this process is thought to facilitate the formation of channels, which increases biofilm formation on the macroscopic level, whereas higher concentrations promote detachment and thus a reduction in biofilm mass (Figure 3B).

Biofilm formation in staphylococci has been shown to be exopolysaccharide dependent or independent (24, 25). To analyze whether PSMβ peptides mediate biofilm detachment in both exopolysaccharide-dependent and –independent *S. epidermidis* biofilms, we first determined presence of the *ica* genes responsible for production of the main biofilm exopolysaccharide polysaccharide intercellular adhesin (PIA, or poly-N-acetylglucosamine [PNAG]) in the 24 *agr*-negative *S. epidermidis* strains. Then we determined in vitro biofilm formation by these strains. Interestingly, biofilm-forming capacity was significantly higher among the strains that contained *ica* genes than among the *ica*-negative strains (Figure 4A), confirming the importance of PIA/PNAG for efficient biofilm formation in *S. epidermidis* (24). We selected the 2 *ica*-negative strains with the highest biofilm-forming capacity and 1 *ica*-positive strain, in addition to strain 1457, to confirm the universal importance of PSMβ peptides for biofilm detachment in vitro. In all strains, PSMβ1 had a biofilm detachment effect very similar to that observed with strain 1457 (Figure 4D), demonstrating that the impact of PSMβ peptides on biofilm detachment in vitro is not dependent on whether biofilm formation is exopolysaccharide dependent or independent.

To confirm the specificity of PSMβ detachment activity and analyze the importance of the PSMβ amphipathic α-helix in the observed detachment process, we synthesized a PSMβ1 derivative, PSMβ1*, in which 5 amino acids were altered to prevent the formation of an amphipathic α-helix (Figure 4, B and C). As the formation of an amphipathic α-helix is the basis of surfactant properties, these experiments were also conducted to gain insight into whether the detachment mechanism is dependent on the surfactant properties of PSMβ1. According to analysis by HeliQuest (http://heliquest.ipmc.cnrs.fr), the amphipathic α-helical part of PSMβ1 extends from amino acids 17 to 44 (C terminus). This was predicted by the hydrophobic face that is characteristic of an amphipathic α-helix and was found for 18–amino acid stretches comprising those, but not amino acids N-terminal of position 17 (stretches 1–18 to 16–43). In the C-terminal part of PSMβ1, 2 lysine residues (positive charge) were changed to proline residues (K22P, K40P), and 3 uncharged amino acids were altered to negatively charged amino acids (W20E, I27E, V35E) to abolish α-helicity and amphipathy in PSMβ1* (Figure 4, B and C). With PSMβ1*, the detachment effect was absent (in strains 1457, BM26, and BM33) or strongly decreased (strain BM32) compared with PSMβ1 (Figure 4D), indicating that the impact of PSMβ1 on biofilm detachment is specific and dependent on the PSMβ amphipathic α-helix. Furthermore, these results strongly suggest that the mechanism by which PSMβ peptides contribute to biofilm maturation and detachment is based on their surfactant properties.

Biofilm structuring and detachment by PSMβ peptides is likely accomplished during biofilm development, while mature *S. epidermidis* biofilms that are stabilized by an exopolysaccharide network may be largely resistant to macroscopic decomposition by externally added PSMβ peptides. To test this hypothesis, we added PSMβ1 peptide at 1 mg/ml to a 24-hour biofilm of the PIA/PNAG-producing strain 1457. We observed only a very minor impact on the biofilm (data not shown). In agreement with a surfactant-based mechanism of PSMβ detachment, these results suggest that PSMβ peptides must be present during biofilm development to promote biofilm structuring and detachment, while the presence of an established matrix network prevents the large-scale detachment of biofilm clusters by PSMβ peptides.

PSMβ peptides promote biofilm structuring and detachment in vitro. To validate the hypothesis that PSMβ peptides promote biofilm detachment, we analyzed biofilm development under flow using confocal laser scanning microscopy (CLSM). To measure expression of the *psm*β operon, we constructed a *psm*β promoter-*egfp* transcriptional fusion. The *egfp* gene was synthetically assembled using codon usage optimized for staphylococci (Supplemental Figure 1; supplemental material available online with this article; doi:10.1172/JCI42520DS1) to increase fluorescence intensity. Expression of *psm*β was limited to the outer layers of the biofilm

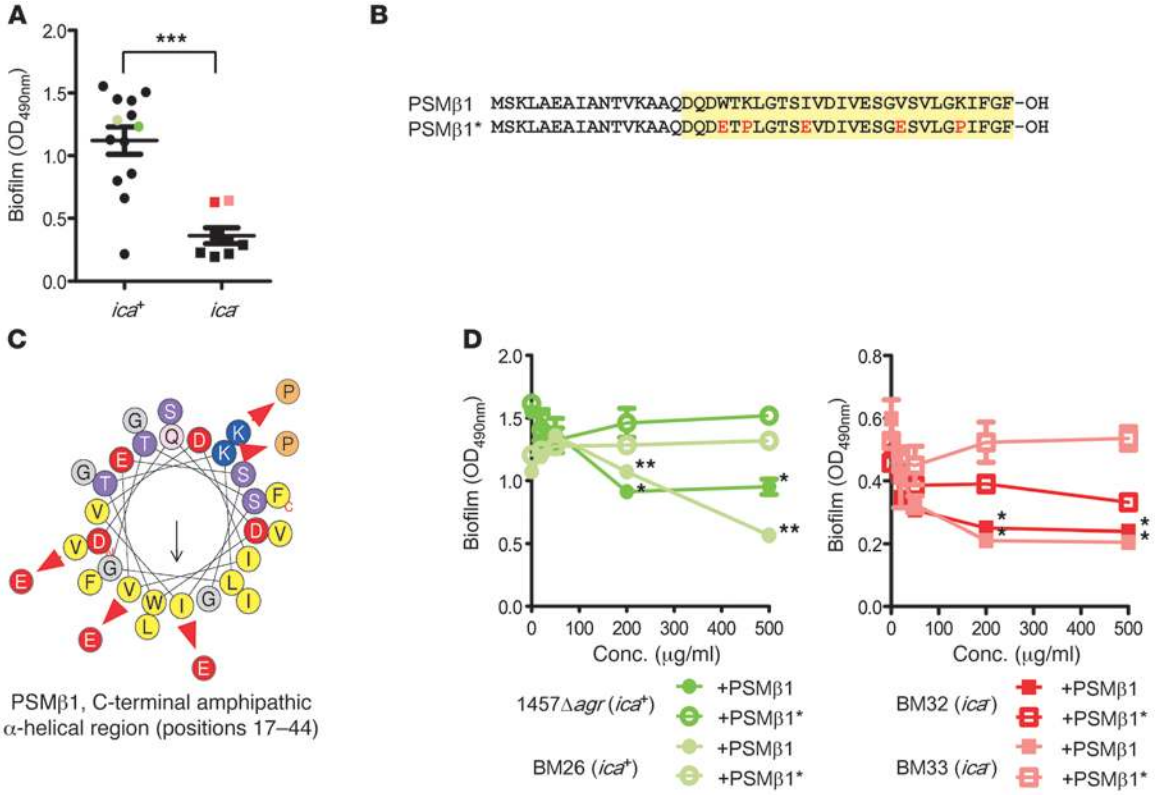

Figure 4

Specific impact of PSMβ1 on in vitro biofilm detachment. (**A**) Biofilm formation by functionally *agr*-negative (without PSM production) *ica*-positive versus *ica*-negative strains. Biofilms were grown in microtiter plates for 24 hours and stained with safranin. ***$P < 0.0001$, *t* test. Colored symbols represent the strains used for the analyses shown in **D**. Error bars depict mean ± SEM. (**B**) α-Helical wheel presentation and (**C**) sequences of PSMβ1 and the mutated PSMβ1* peptide. The α-helical part (positions 17–44) is shaded in yellow. In the sequence, amino acids changed in PSMβ1* in comparison with PSMβ1 are shown in red; in the wheel presentation, exchanges are shown using red arrows. (**D**) Impact of PSMβ1 versus PSMβ1* on in-vitro biofilm development by 2 *ica*-positive and 2 *ica*-negative *S. epidermidis* strains. Conditions are the same as those used for the experiment shown in Figure 3A. *$P < 0.05$; **$P < 0.01$, *t* tests comparing values for the PSMβ1- versus PSMβ1*-treated samples at corresponding concentrations of added peptide.

(Figure 5A) in accordance with a function in detachment and control by *agr*, for which we have previously shown a similar spatial expression pattern in *S. epidermidis* biofilms (26). Importantly, we observed that strong *psm*β expression was followed by the appearance of void spaces (Figure 5, B and C). Furthermore, there were significantly more *psm*β-expressing cells in the effluent compared with the biofilm cells (Figure 5D). These results confirmed our hypothesis that *psm*β expression leads to biofilm cluster detachment during biofilm development.

To further investigate the role of PSMβ peptides in *S. epidermidis* biofilm development, we constructed a deletion mutant of the entire *psm*β operon in *S. epidermidis* 1457 (Figure 2A). CLSM images revealed that static biofilms of the *psm*β operon deletion mutant in comparison with the isogenic WT strain lacked channel formation and were thicker (Figure 6, A and C). Genetic complementation restored the phenotype observed in the WT (Figure 6A). Image analysis of the biofilms using IMARIS software showed a significant increase in the total and average biovolumes, indicative of an increase in total biofilm formation and decrease in the degree of channel formation, respectively, comparing the mutant to the WT, while complementation restored WT levels (Figure 6B). These findings showed that PSMβ peptides promote channel formation in *S. epidermidis* biofilms. In addition, they further substantiated that PSMβ peptides facilitate detachment, as the lack of detachment leads to biofilm expansion.

Furthermore, we compared the phenotype of the *psm*β deletion mutant with that of an isogenic *agr* mutant. The biofilm phenotypes of these strains were very similar (Figure 6C), indicating that PSMβ peptides represent the main effector molecules of quorum-sensing regulated biofilm maturation in *S. epidermidis*.

PSMβ peptides promote dissemination from in vivo biofilms. To analyze the role of β-type PSMs in biofilm detachment in vivo, we performed a murine model of device-related infection (Figure 7 and Table 1). The development of human sepsis is a rare event compared with the frequency of catheter infection and possibly due to yet unknown roles of host factors; it is thus difficult to mimic in an animal model. We therefore focused on analyzing bacterial spread from the catheters to the lymph and organs. Furthermore, we used immune-compromised Nu/Nu mice, as we showed previously that those mice develop more pronounced and longer lasting catheter-related infection (27).

In this model, 2 catheters, precolonized with equal numbers of either the *psm*β mutant or WT strain, were inserted s.c. on the right and left dorsum, respectively. In a first experiment, we measured systemic dissemination into body fluids as assessed by taking body

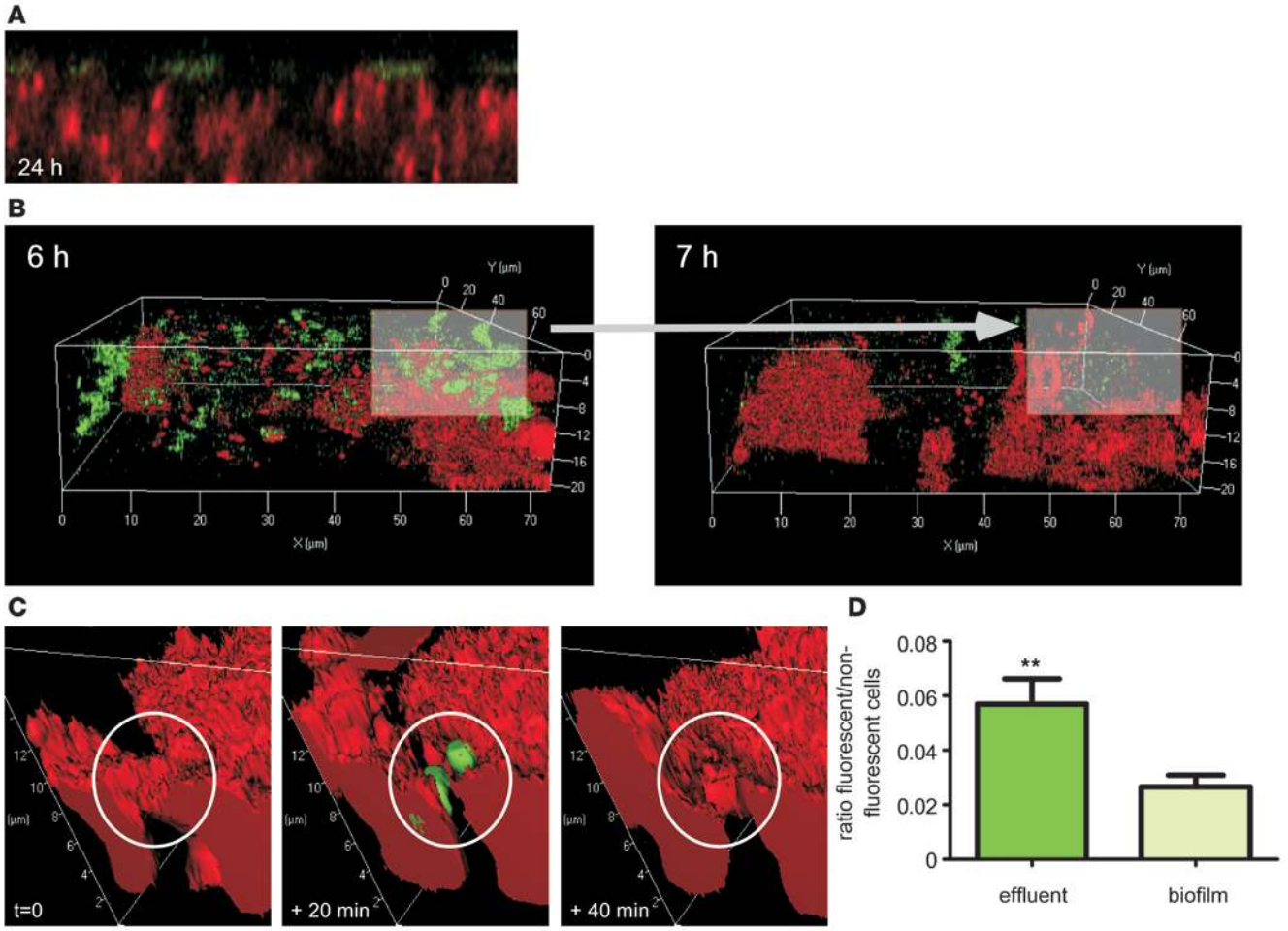

Figure 5
Role of PSMβ peptides in *S. epidermidis* biofilm development: cell detachment. A *psm*β-promoter *egfp* fusion construct (see Supplemental Figure 1 for the synthetic *egfp* gene with optimized *Staphylococcus* codon usage) was produced to monitor *psm*β expression in dynamic *S. epidermidis* biofilms using flow cells with CLSM (green). Entire biofilms were stained with propidium iodide (red). (**A**) Mature (24 hours) biofilm showing expression of *psm*β at the outer biofilm layer. (**B** and **C**) Biofilm cluster detachment observed during biofilm development. Lower (**A**) and higher (**B**) temporal and spatial resolution is shown. (**D**) Comparative analysis of the relative amount of cells expressing *psm*β (green fluorescence) in effluent and biofilm. The ratio of fluorescent versus nonfluorescent cells was determined using IMARIS software in effluent and biofilm samples. $^{**}P < 0.01$, *t* test. Error bars depict mean ± SEM.

fluid samples from the peritoneal cavity. Bacteria harvested from body fluids were overwhelmingly and significantly more of the WT than *psm*β mutant strain (Table 1), indicating dissemination is favored in the WT over the mutant strain. Bacteria were rarely found in organs, but those that were found were almost exclusively of the WT. Owing to low and strongly varying numbers, differences in the organs only reached statistical significance in the liver sample at day 4 (Table 1). Finally, bacteria on the WT infected catheter were only of the WT strain, while on the *psm*β mutant–infected catheter, rare infiltration of WT bacteria was detected, in accordance with dissemination occurring only for WT bacteria.

In a second experiment, we focused on determining bacterial dissemination into the lymph nodes, as those would be first encountered by bacteria after dissemination. Bacteria in all lymph nodes were almost exclusively of the WT strain (Figure 7 and Table 1). Only bacteria in the right brachial and axillary lymph nodes were mainly of the mutant strain, most likely due to involvement of adjacent tissue during surgical insertion of the catheters. In contrast, no bacteria were found in the blood. This suggests that bacteria found in the body fluids from the peritoneal cavity in the first experiment originated from the lymph, while host defenses had cleared bacteria in the blood. Together, these data demonstrated that systemic dissemination from the indwelling device was strongly and significantly favored in the WT compared with the *psm*β deletion strain and thus, PSMβ peptides play a key role in the dissemination of biofilm-associated infection. Finally, results from a bacteremia control experiment indicated that PSMβ peptides do not have an impact on the development of disease that is unrelated to biofilm formation, as no significant difference was detected when monitoring death of animals injected with WT or *psm*β mutant bacteria, respectively (Supplemental Figure 2).

Antibodies to PSMβ peptides block dissemination of biofilm-associated infection. To further substantiate the involvement of PSMβ peptides in the dissemination of biofilm-associated infection,

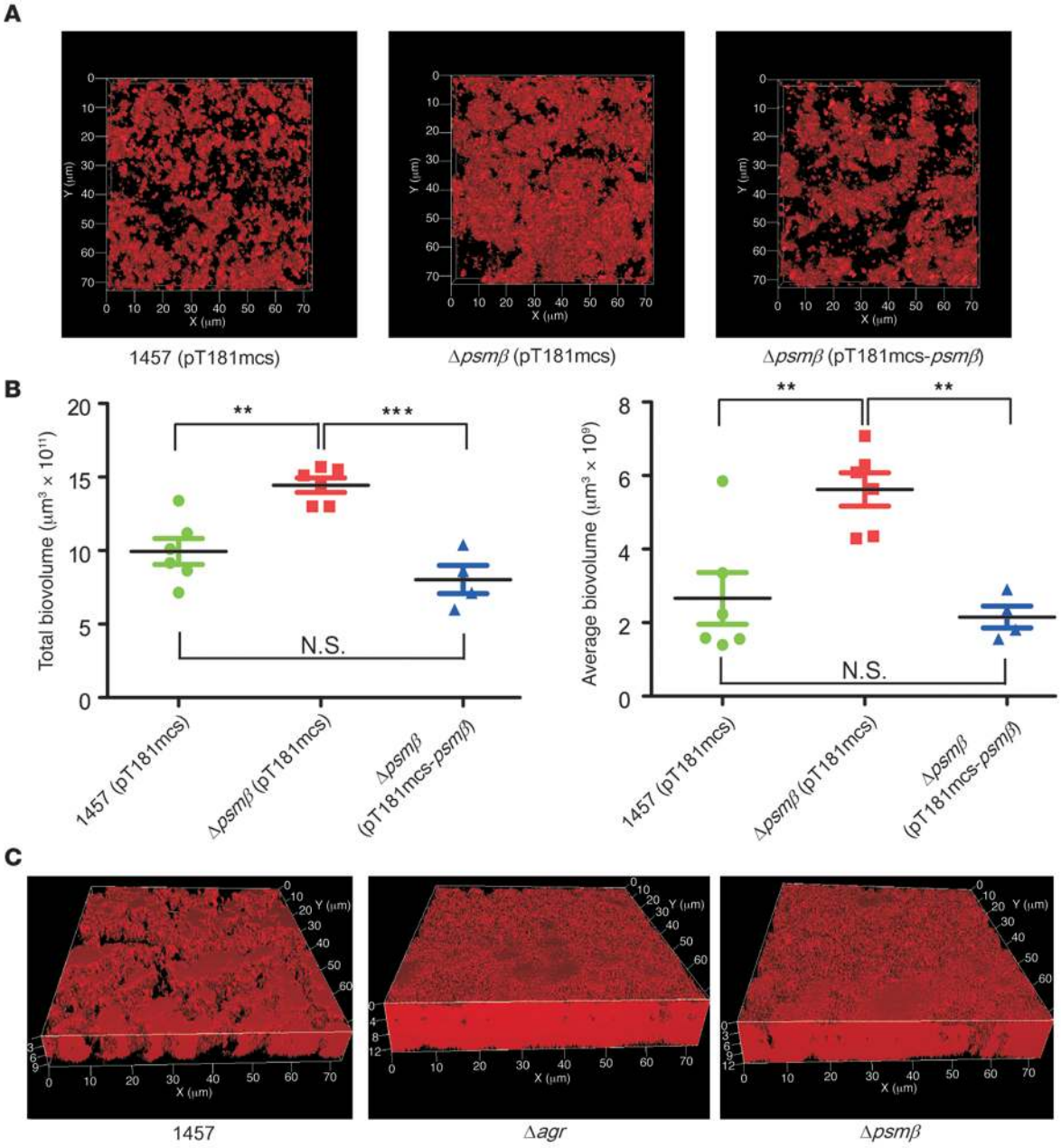

Figure 6

Role of PSMβ peptides and *agr* in *S. epidermidis* biofilm development: channel formation and biofilm expansion. (**A**) CLSM pictures of *S. epidermidis* 1457 WT, isogenic *psm*β mutant, and *psm*β-complemented strains. The WT and *psm*β mutant strains were transformed with the control plasmid pT181mcs to ensure comparability. Static biofilms were grown for 24 hours, stained with propidium iodide, and imaged using CLSM. View is from the top. (**B**) Analyses of total and average biovolumes, which are measures of total biofilm and degree of channel formation, respectively, using IMARIS software of the biofilm samples shown in part **A**. Note that increased average biofilm volume corresponds to decreased channel formation. $^{**}P < 0.01$; $^{***}P < 0.001$, 1-way ANOVA with Bonferroni's post tests. Error bars depict mean ± SEM. (**C**) CLSM pictures of *S. epidermidis* 1457 WT, isogenic *agr*, and *psm*β operon deletion mutant biofilms. Growth conditions are as in **A**.

we investigated whether antibodies against PSMβ peptides prevent dissemination. To that end, we first produced antibodies to PSMβ1 and PSMβ2 in mice. PSMβ peptides proved immunogenic and elicited a strong IgG response (Supplemental Figure 3). Antisera were treated using extracts from the *psm*β deletion mutant, and the resulting blocked antisera were highly specific for PSMβ1 and PSMβ2, respectively (Supplemental Figure 3). We pooled the PSMβ1 and PSMβ2 antisera and analyzed the efficacy of the obtained serum in reducing the dissemination of biofilm-associated infection using the same device-related infection model. In contrast to animals treated with PBS or control serum, no bacteria were found in the livers, spleens, or kidneys of animals treated with the anti-PSMβ antibodies, and bacterial load in the lymph nodes was significantly reduced (Figure 8). Reduced bacte-

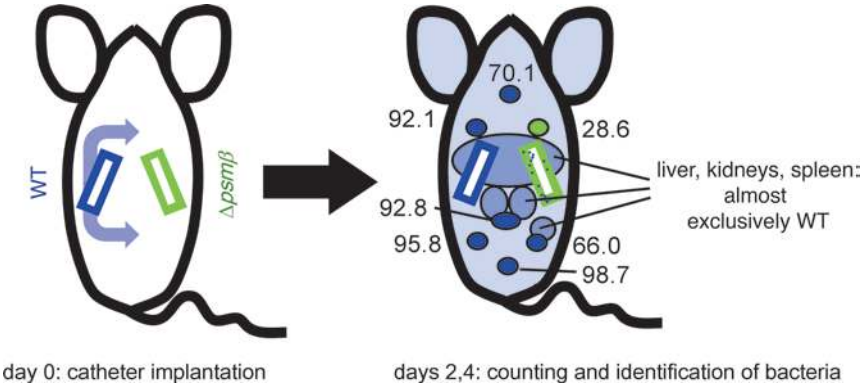

Figure 7
Role of PSMβ peptides in the dissemination of biofilm-associated infection. Catheter pieces with equal cell numbers of preformed biofilms of either the *S. epidermidis* 1457 WT or isogenic *psm*β mutant strains were inserted under the skin of mice at the dorsum. Each mouse received 2 pieces, left and right, 1 of which was coated with WT and 1 with mutant biofilms. At days 2 and 4 after insertion (this timing found in a pilot experiment to be optimal), catheter pieces were removed and dissemination was analyzed. In a first experiment, body fluids (from the i.p. cavity) and organs were analyzed. Almost all disseminated bacteria detected were of the WT, and significantly more WT than mutant bacteria were detected in the body fluids and liver. Number of mice: $n = 9$ (day 2); $n = 6$ (day 4). In a second experiment, lymph nodes at day 2 after infection were analyzed and showed predominantly WT bacteria, except for in the nodes adjacent to the catheter infected with *psm*β mutant bacteria. Numbers represent percentages of WT among total bacteria from all tested mice ($n = 7$) in the respective lymph nodes. Blue, WT; green, *psm*β mutant strains. See Table 1 for details.

rial counts were most likely not due to an opsonophagocytosis-enhancing effect of the anti-PSMβ antibodies, as in an in vitro control experiment, we did not observe enhanced bacterial killing with anti-PSMβ compared with control serum (Supplemental Figure 4). Thus, these results confirmed that PSMβ peptides are essential for the dissemination of biofilm-associated infection.

Discussion

In the present study, we show that biofilm maturation and detachment in *S. epidermidis* are mediated by a specific class of surfactant peptides, the β-type PSMs. Notably, these findings provide a mechanistic basis for crucial steps in staphylococcal biofilm development that were not previously understood on a molecular level. Furthermore, using a premier biofilm-forming pathogen, our results lend support to the evolving concept that biofilm maturation in bacteria is accomplished by the use of surfactants (7–10). However, it is important to note that the various bacterial systems appear to share only the surfactant physicochemical properties of the biofilm maturation effectors and quorum-sensing control of their production. In contrast, the chemical nature of the surfactants and genetic basis of their biosynthesis are completely unrelated.

Detailed understanding of the molecular determinants governing biofilm development is of utmost importance for potential therapeutic interference with biofilm-associated infection. In biofilm-forming pathogens, biofilm detachment processes have exceptionally high significance, as they are believed to lead to the systemic dissemination of infection. However, molecular effectors of biofilm maturation and detachment have not been analyzed in vivo in any biofilm-forming pathogen. It is therefore important to stress that our study establishes in vivo relevance for biofilm detachment by demonstrating a key role of surfactant-like peptides in promoting the dissemination of *S. epidermidis* biofilm-associated infection.

Biofilm maturation and detachment are commonly under quorum-sensing regulation to ascertain a well-controlled degree of channel formation and biofilm expansion (12, 26, 28, 29). This is also the case for staphylococci (26, 28–31). Importantly, our findings indicate that the PSMβ peptides are the main determinants that exert the impact of quorum-sensing control on these mechanisms of biofilm development in *S. epidermidis* on the molecular level. This is in good agreement with our previous observation in *S. aureus* showing that the mechanism of *psm* control by *agr* is different from, and likely evolved before, *agr* control of other staphylococcal virulence determinants (16). Our finding that PSMs have a key role in biofilm development as a basic phenotype of staphylococcal physiology during both commensal life and infection provides a plausible explanation for the stringency and early evolution of that regulation. Interestingly, the relatively higher concentration of PSMβ peptides compared with other PSM peptides in biofilm versus planktonic culture indicates that the *psm*β operon is regulated by a yet unknown regulator in addition to the *psm* master regulator *agr*. Furthermore, we have previously shown that Agr-dysfunctional and thus, PSM-negative strains are more frequently found among strains isolated from biofilm-associated infection (26). Our present results suggest that such strains have lost the capacity to detach and owing to the lack of PSMβ production may form more compact and extensive biofilms.

Blocking the *agr* quorum–sensing system has been frequently proposed as a potential basis for novel therapeutics interfering with staphylococcal virulence, as many toxins are under positive control of *agr* (32–34). On the other hand, it has been noted that this may lead to increased biofilm formation, owing to negative *agr* control of biofilm expansion (33), which is in accordance with results achieved in the present study. However, our results also indicate that such treatment may inhibit bacterial dissemination from biofilms, showing that interference with *agr* might potentially be beneficial also during biofilm-associated infection. In addition, we provide proof of principle that the specific inhibition of biofilm detachment surfactants may prevent dissemination, a strategy we believe should be further evaluated for potential therapeutic use.

Surfactants are not the only molecules that have been proposed to contribute to biofilm maturation and detachment in staphylococci. According to an alternative hypothesis, these processes may also be accomplished by enzymatic degradation of biofilm matrix molecules. In that regard, recent research indicated that staphylococcal biofilm formation is accomplished by protein and/or exopolysaccharide biofilm matrix components (24, 25). Hypothetically, enzymatic degradation of these polymers may thus contribute to biofilm maturation; and a proteolytic detachment mechanism has been proposed for protein-dependent biofilms of *S. aureus* (28). However, direct evidence for such a mechanism is scarce and no evidence has been produced for clinical strains or in vivo. Furthermore, it has been shown that such enzymes specifically degrade only those staphylococcal biofilms that are

Table 1
Catheter-related animal infection model

Analyzed organ, body, fluid or tissue	Day 2, total numbers ($n = 9$, except for lymph nodes[A])	Day 4, total numbers ($n = 6$)	Percentage WT bacteria among total, day 2[B]	Percentage WT bacteria among total, day 4
Catheter, WT side (left)	$1.29 \pm^{C} 0.42 \times 10^5$	$0.67 \pm 0.46 \times 10^5$	99.8	100
Catheter, Δ*psm*β side (right)	$1.02 \pm 0.42 \times 10^5$	$1.09 \pm 0.49 \times 10^5$	6.3	6.1
Blood/body fluids (i.p. cavity)	$1.2 \pm 0.43 \times 10^3$/ml	$1.1 \pm 0.46 \times 10^3$/ml	97.2 ($P < 0.0001^{D}$)	98.1 ($P < 0.0001$)
Liver	100 ± 57	150 ± 33	93.3	96.7 ($P = 0.045$)
Kidney	17 ± 4	42 ± 12	100	96.0
Spleen	31 ± 22	20 ± 4	96.6	91.9
Blood[A] (heart puncture)	0	ND		
Lymph nodes ($n = 7$[A])				
Brachial/axillary, left (WT side)	$0.33 \pm 0.10 \times 10^3$	ND	92.1	ND
Brachial/axillary, right (Δ*psm*β side)	$1.31 \pm 0.36 \times 10^3$	ND	28.6	ND
Cervical	$2.12 \pm 1.48 \times 10^3$	ND	70.1	ND
Inguinal, left (WT side)	$0.10 \pm 0.10 \times 10^3$	ND	95.8	ND
Inguinal, right (Δ*psm*β side)	$0.21 \pm 0.12 \times 10^3$	ND	66.0	ND
Paravertebral	$0.80 \pm 0.74 \times 10^3$	ND	98.7	ND
Mesenteric	$2.18 \pm 1.41 \times 10^3$	ND	92.8	ND

[A]Dissemination into lymph nodes and blood was investigated in a separate experiment under the same experimental conditions. [B]Fifty-two clones, or the total number of available clones, were assayed for spectinomycin sensitivity to calculate WT versus Δ*psm*β percentages. [C]SEM. [D]Statistics: WT versus Δ*psm*β bacteria, unpaired *t* tests.

based on proteins, or exopolysaccharides, respectively (35). Moreover, it has become clear that staphylococci do not produce an enzyme to degrade the PIA/PNAG exopolysaccharide, the most well-established staphylococcal biofilm matrix component (36). It is therefore important to stress that, in contrast, our results indicate that the PSM-based surfactant detachment mechanism is largely independent of the biofilm matrix chemical composition. Finally, presence of PSMs and PSM-like molecules in many staphylococci including *S. aureus* (18, 37, 38) indicates that PSMs may also contribute to biofilm structuring in other staphylococcal species, which remains to be investigated.

In summary, our study presents a mechanism of *S. epidermidis* biofilm maturation and detachment that is likely used in a similar form by other staphylococcal biofilm–forming strains. Furthermore, using *S. epidermidis* as an example, our study provides evidence for the importance of biofilm detachment molecules in the dissemination of biofilm-associated infections, thus identifying a potential target for therapeutics aimed at preventing complication and spread of such infections.

Methods

Bacterial strains, plasmids, and growth conditions. *S. epidermidis* 1457 is a biofilm-forming clinical isolate frequently used for biofilm research (21). The *S. epidermidis* 1457 *psm*β mutant was constructed by replacement with a spectinomycin cassette as described (39, 40) (for all oligonucleotides, see Table 2). Fidelity of the deletion was determined by DNA sequencing and reversed phase HPLC/electrospray ionization mass spectrometry (RP-HPLC/ESI-MS) of culture supernatants, which demonstrated the specific absence of the PSMβ peptides. For complementation, the *psm*β operon from *S. epidermidis* 1457 was PCR amplified and cloned in plasmid pT181mcs (41). The *psm*β promoter *egfp* fusion was produced by cloning the putative *psm*β promoter in front of an *egfp* gene that was synthesized with optimized codon usage for staphylococci (Supplemental Figure 1). Bacteria were grown in tryptic soy broth (TSB) to which 0.5% glucose was added for biofilm experiments. Antibiotics were added when appropriate (12.5 μg/ml tetracycline, 400 μg/ml spectinomycin, 10 μg/ml chloramphenicol). Spectinomycin was only used during construction of, but not in experiments using, the *psm*β deletion strain.

*Analytical PCR to test for presence of psm*β *and ica genes*. Genomic DNA was isolated from all *S. epidermidis* strains that did not show PSM peaks in HPLC analysis. The strain collections originated from Paris and Shanghai (42, 43). Presence of *psm*β genes was tested using primers designed to amplify both *psm*β*1* and *psm*β*2*, and either *psm*β*1* or *psm*β*2* alone (Table 2). Strains showing at least 1 positive signal were regarded as positive for the *psm*β locus. One strain showing no signal was determined not to be *S. epidermidis* by Api Staph (bioMérieux) analysis. Presence of *ica* genes was determined using primers icaBF and icaBR, which amplify a portion of the *icaB* PIA/PNAG deacetylase gene (44).

s.c. device–related biofilm infection model. Segments of i.v. catheters (Abbott Ireland), 1.0 cm in length, were precolonized with overnight cultures of *S. epidermidis* 1457 or the isogenic *psm*β deletion strain for 3 hours at 37°C. After precolonization, each catheter segment was rinsed with 2 ml sterile PBS and air dried to remove residual bacterial cultures. Bacteria on several catheter pieces that were treated equally to those inserted in the animals were counted (using the method described below), showing that equal numbers of WT and mutant bacteria adhered. Nu/Nu B/C CRL female mice (Charles River Laboratories) weighing 18–25 g were anesthetized with isoflurane, their flanks shaved, and the skin cleansed with betadyne and ethanol. A 5.0-mm incision was made and dissected to create a s.c. tunnel into which a precolonized catheter segment was implanted at a distance of at least 2 cm from the incision. The incision was closed with surgical sutures and the skin disinfected. Two catheter segments were inserted into each animal, 1 on each side, 1 precolonized with *S. epidermidis* 1457, and the other with the isogenic *psm*β deletion strain. After catheter implantation, animal general health condition and disease advancement were monitored every 24 hours for a total of 4 days. Animals were euthanized via exsanguinations under deep surgical anesthesia (isoflurane) either on day 2 or day 4 after catheter implantation. Animal organs (kidneys, livers, spleens) and implanted catheters or lymph nodes were harvested for further analysis. Animal body fluid samples were obtained from the peritoneal cavity after organ removal. Pure blood samples were obtained via heart puncture. Each harvested catheter

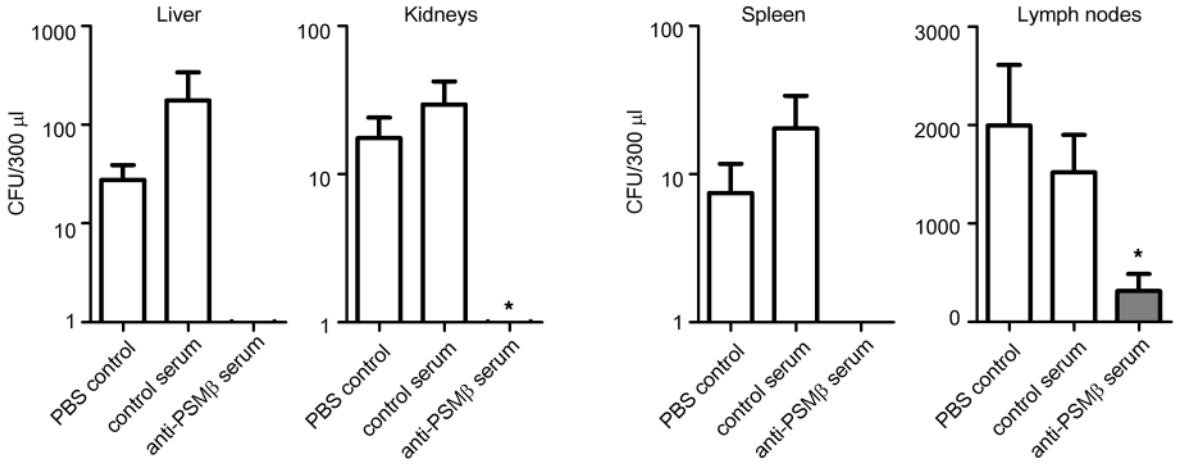

Figure 8
Blocking dissemination of biofilm-associated infection using anti-PSMβ serum. Specific antisera against PSMβ1 and PSMβ2 were mixed 1:1 and used to protect mice in the biofilm infection/dissemination model. *$P < 0.05$, versus PBS and control serum for the lymph nodes, versus PBS for the kidney results; 1-way ANOVA with Bonferroni's post-tests. For spleen and liver, differences were not statistically significant owing to the fact that dissemination into organs only occurred in a limited number of mice and therefore SEM values were high. However, dissemination into the organs of mice that received anti-PSMβ serum was never observed (average CFU/100 μl ≤ 1). Number of mice: controls, $n = 9$; anti-PSMβ, $n = 7$. Control serum was from animals that received injections containing CFA and IFA. Error bars depict mean ± SEM.

was rinsed with 2 ml sterile saline, air dried, then sonicated in 1 ml sterile saline for 1 minute, and vigorously vortexed for 10 minutes to remove bacterial cells from the catheter. Obtained cell solutions were diluted 1:10. Each organ was ground in 3 ml saline using a conical tissue grinder (VWR). Lymph nodes (only harvested at day 2 after infection) were surgically excised and ground using disposable pellet pestles in 100 μl saline. The left and right brachial/axillary and the inguinal lymph nodes were analyzed separately, while the cervical nodes were combined for analysis. Then 100 μl of all obtained solutions, blood, or body fluid samples were plated on TSB plates and counted. Colonies were transferred to TSB plates containing 400 μg/ml spectinomycin in order to distinguish colonies of the *psm*β mutant strain (spectinomycin resistant) from those of the WT strain, and percentages of each colony type were determined. For passive immunization, each mouse received 100 μl of purified mouse anti–PSMβ-IgG via i.p. injection. Control animals received injections of sterile PBS or purified serum IgG obtained from BALB/c mice immunized with adjuvant only. Precolonized catheters were s.c. inserted into the animals 24 hours after passive immunization. The infection model was performed as above, except both catheter pieces were colonized with WT bacteria, and bacterial loads were determined in the organs and lymph nodes. All animal protocols were reviewed and approved by the Animal Use Committee at Rocky Mountain Laboratories, NIAID, NIH.

Opsonophagocytosis assay. An overnight culture of *S. epidermidis* 1457 was inoculated at an OD_{600nm} of 0.1 into 50 ml of TSB (in 125 ml conical glass flasks) at 37°C and grown for 3 hours. The bacteria were washed once in ice-cold PBS and then harvested by centrifugation at 4°C. Dilutions of bacteria in PBS were opsonized with purified mouse antibodies against PBS or PSMβ1/PSMβ2 in a 1:1 ratio for 30 minutes at 37°C. Female Nu/Nu B/C CRL mice (Charles River Laboratories) were exsanguinated. The obtained mouse blood was incubated for 60 minutes at 37°C with the opsonized bacteria at a ratio of antibody/bacteria/blood of 1:1:16 in a total volume of 100 μl. In preliminary experiments, a bacterial dose of 5×10^4 was determined to be optimal, as the

Table 2
Oligonucleotides used in this study

Oligo name	Oligo sequence
Construction of Δ*psm*β mutant	
Betasac	GAAACTTTTGCTGAGCTCGTATACAAGGATCATGAAAATACC
Betabam	CTCCAAAACGATTGGATCCGATTGCGATTCG
Betasal	GTAGAAAGTGGCGTTAGCGTATTAGGTCGACTCTTCGG
Betapst	CAAGCGTTGGCTCAACTTACACTGCAGCAATTGTC
***psm*β complementation plasmid**	
22N	GTAAAACCTAAGAAAATTAACAGTTAGGAATTCTTAATTATTTAG
28N	GCTTTTTTCTCAGCATCATAAGGATCCACTAATGTATCGTCG
Cloning of *psm*β promoter region in *egfp* fusion vector	
22N	GTAAAACCTAAGAAAATTAACAGTTAGGAATTCTTAATTATTTAG
Egfpbeta3bam	GCGGGTTTTAATCTCTGTTGAATTCTATTATTGTATTTTAC GCGTTAAATAATTTCATTATTAAGGATCCTAAATG
Probe for Northern blot	
PSMβ probe	GCGGGTTTTAATCTCTGTTGAATTCTATTATTGTATTTTAC
Oligonucleotides to test for presence of *psm*β genes	
Amplifying parts of *psmβ2* and *psmβ3*	
PSMβtestfor	TATTTGACGCAATTAGAAGTGTAG
PSMβtestrev	GCTAACGCCACTTTCTACGATGTC
Amplifying parts of *psmβ2* and *psmβ1*	
PSMβ1bfor	TTAGCAGAAGCTATTGCAAATACA
PSMβ1arev	TTAGAAACCGAAGATTTTACCTAATACGCT
Amplifying parts of *psmβ3*	
PSMβtestfor	TATTTGACGCAATTAGAAGTGTAG
PSMβ2rev	AATAATTTAGAAATAATACTAACA

largest difference between control (blood) and antibody-treated samples was observed at that dose. Surviving bacteria were counted by spotting 400 μl (16 × 25 μl aliquots) onto TSB plates.

CLSM. For static biofilm assays, 300 μl TSB/0.5 % glucose was inoculated from precultures grown overnight at a dilution of 1:100 in 8-well polystyrene chambers (Lab-Tek II; Nunc). After 24 hours of incubation at 37°C, supernatants were gently removed, and biofilm layers were washed twice with PBS, resuspended in 400 μl PBS, and stained with propidium iodide (4 μM, 400 μl, 10 minutes). Flow cells (Stovall FLCAS0001) were inoculated from precultures grown overnight, cells were let to settle for 1 hour, and biofilms were grown under a constant flow of TSB/0.5% glucose/4 μM propidium iodide, using an Ismatec IP Precision Pump at setting 9.0. Images were acquired on a Zeiss LSM 5 Pascal laser-scanning confocal unit equipped with an argon laser, a helium-neon laser, and an Axiovert 100 microscope (Zeiss) with a 63 × 1.4–NA oil-immersion objective. Zeiss 3D (Image VisArt) software was used for the 3D visualization of biofilm structures. Further image analysis was performed using IMARIS 7.0.0 software (Bitplane).

Synthesis and detection of PSM peptides. PSM peptides were synthesized by a commercial vendor at a purity of greater than 95% with the naturally occurring N-terminal N-formyl methionine present. RP-HPLC/ESI-MS was used to measure PSM concentrations in culture filtrates as described previously (17) with slight modifications. An Agilent Technologies Zorbax SB-C8 2.3 × 30 mm reversed-phase column was used. A gradient from 0.1% trifluoroacetic acid in water to 0.1% trifluoroacetic acid in acetonitrile was run at a flow rate of 0.5 ml/min. The LC-MS system consisted of an Agilent 1100 series HPLC system connected to an Agilent Trap VL Ion Trap–Type Mass Spectrometer. 10 or 100 μl culture filtrate was injected for each sample run. Calibration was performed using synthetic PSM peptides. The 2 major peaks of each PSM ESI mass spectrogram were used to compute PSM concentrations using Agilent Quant Analysis Software.

Generation, purification, and determination of immunogenicity of PSMβ-specific mouse antisera. To generate *S. epidermidis* PSMβ peptide–specific antibodies, BALB/c female mice (6–8 weeks / 20–25 g; Charles River Laboratories) were s.c. injected with 50 μg of N-formylated PSMβ1 or PSMβ2 in 100 μl sterile PBS emulsified with CFA for primary immunization. Two booster immunizations, which contained incomplete Freund adjuvant (IFA) instead of CFA, were given to the mice on day 14 and day 28 after the primary immunization. The control animals received injections of sterile PBS and adjuvant only. Blood samples were collected before each immunization. All animals were sacrificed 14 days after the second booster immunization for the terminal blood samples. Serum samples were collected for peripheral blood antibody evaluation. To block nonspecific binding, anti-PSMβ1 and anti-PSMβ2 sera were pooled, diluted 1:50 in TBS buffer (Tris-buffered saline: 10 mM Tris-HCl, 150 mM NaCl, pH 7.4), and incubated with overnight culture supernatant of the *S. epidermidis* 1457 isogenic *psm*β deletion strain for 16 hours at 4°C with gentle shaking. Precipitated material was sedimented by centrifugation at 28,000 *g* for 30 minutes at 4°C, and PSMβ-specific IgG in the supernatant was purified using a HiTrap Protein G Affinity Column (GE Healthcare). Control serum samples obtained from animals immunized with adjuvants only were purified following the same procedure. The eluted IgG fractions were concentrated using Amicon Ultra-15 centrifugal filter units (Millipore) and dialyzed against sterile PBS using Slide-A-Lyzer Dialysis Cassettes (Thermo Scientific).

ELISA assays with synthetic *S. epidermidis* PSMβ peptides were used to determine whether the peptides were immunogenic. Microtiter plates (Nunc 96-well flat-bottom MaxiSorp plates) were coated with 20 μg/ml of each synthetic PSMβ peptide in PBS plus 0.05% NaN_3 and incubated overnight at 4°C. The plates were washed with PBS containing 0.05% Tween-20 and blocked for 1 hour at room temperature with 1% BSA (Sigma-Aldrich) and 0.05% NaN_3 in PBS. Serum samples were diluted in assay diluent (Tris-buffered saline containing 0.1% BSA and 0.05% Tween-20, pH 7.2) and added to the washed wells at 100 μl/well for an incubation of 2 hours at room temperature. Plates were washed again and HRP-labeled goat anti-mouse IgG (R&D Systems) or goat anti-mouse IgM (Jackson ImmunoResearch Laboratory) were diluted in assay diluent and added to the plates at 100 μl/well for an incubation of 1 hour at room temperature in order to detect PSMβ1- or PSMβ2-specific mouse IgG and IgM, respectively. Plates were washed again and a substrate solution containing equal volumes of tetramethylbenzidine and H_2O_2 was added to the plates at 100 μl /well for color development. The reaction was terminated by adding 50 μl of 1 M H_2SO_4 to each well, and OD was measured at 450 nm using an ELISA plate reader.

Northern blot analysis. Total RNA (10 μg) was prepared from mid-log, late-log, and stationary growth phase of *S. epidermidis*, electrophoresed in an formaldehyde agarose gel (1.2%), transferred to a nylon membrane, and cross-linked with UV radiation. The DNA probe was PCR generated using specific primers (Table 2), covering the entire *psm*β operon from *psm*β*1* to *psm*β*3*, and labeled with digoxigenin (DIG) using a Roche DIG labeling kit according to the manufacturer's instructions. The hybridized probe was incubated with an alkaline-phosphatase–conjugated anti-DIG antibody and detected using NBT/BCIP.

Microtiter plate biofilm assays. In vitro biofilm assays were performed in 96-well polystyrene microtiter plates as described previously (31). Plates were incubated after inoculation at 37°C for 24 hours without shaking. Biofilm formation was made visible by staining with 0.1% safranin (Sigma-Aldrich) for 30 seconds and quantified using a Safire microtiter plate reader (Tecan) and Magellan Version 3.00 software (Tecan). The reader was set to multiple read mode (circle pattern, 6 × 6 number of reads), and absorbance was measured at 490 nm.

Statistics. 1-way ANOVA with Bonferroni's post-tests or unpaired *t* tests was used to calculate 2-tailed *P* values using Graph Pad Prism 5 software. $P < 0.05$ was considered significant. Error bars depict mean ± SEM.

Acknowledgments

This study was supported by the Intramural Research Program of the National Institute of Allergy and Infectious Diseases (NIAID), NIH. The authors thank Frank DeLeo for critically reading the manuscript, Saravanan Periasamy, NIAID, for help with confocal microscopy, and Daniel C. S. Tan, Nanyang Polytechnic, Singapore, for technical assistance.

Received for publication February 1, 2010, and accepted in revised form October 20, 2010.

Address correspondence to: Michael Otto, National Institute of Allergy and Infectious Diseases, NIH, 9000 Rockville Pike, Building 33 1W10, Bethesda, Maryland 20892, USA. Phone: 301.443.5209; Fax: 301.480.3633; E-mail: motto@niaid.nih.gov.

Rong Wang's present address is: Meat Safety and Quality Research Unit, U.S. Meat Animal Research Center, Clay Center, Nebraska, USA.

Shu Y. Queck's present address is: Nanyang Polytechnic, Singapore.

Kok-Fai Kong's present address is: Department of Cell Biology, La Jolla Institute for Allergy and Immunology, La Jolla, California, USA.

Max Jameson-Lee's present address is: Myles Thaler Center, University of Virginia, Charlottesville, Virginia, USA.

Burhan A. Khan's present address is: Southcentral Foundation, Anchorage, Alaska, USA.

1. Costerton JW, Stewart PS, Greenberg EP. Bacterial biofilms: a common cause of persistent infections. *Science*. 1999;284(5418):1318–1322.
2. Mah TF, O'Toole GA. Mechanisms of biofilm resistance to antimicrobial agents. *Trends Microbiol*. 2001;9(1):34–39.
3. Otto M. *Staphylococcus epidermidis* - the 'accidental' pathogen. *Nat Rev Microbiol*. 2009;7(8):555–567.
4. Rogers KL, Fey PD, Rupp ME. Coagulase-negative staphylococcal infections. *Infect Dis Clin North Am*. 2009;23(1):73–98.
5. Stoll BJ, et al. Late-onset sepsis in very low birth weight neonates: the experience of the NICHD Neonatal Research Network. *Pediatrics*. 2002; 110(2 pt 1):285–291.
6. O'Toole G, Kaplan HB, Kolter R. Biofilm formation as microbial development. *Annu Rev Microbiol*. 2000;54:49–79.
7. Branda SS, Gonzalez-Pastor JE, Ben-Yehuda S, Losick R, Kolter R. Fruiting body formation by *Bacillus subtilis*. *Proc Natl Acad Sci U S A*. 2001;98(20):11621–11626.
8. Angelini TE, Roper M, Kolter R, Weitz DA, Brenner MP. *Bacillus subtilis* spreads by surfing on waves of surfactant. *Proc Natl Acad Sci U S A*. 2009; 106(43):18109–18113.
9. Boles BR, Thoendel M, Singh PK. Rhamnolipids mediate detachment of *Pseudomonas aeruginosa* from biofilms. *Mol Microbiol*. 2005;57(5):1210–1223.
10. Davey ME, Caiazza NC, O'Toole GA. Rhamnolipid surfactant production affects biofilm architecture in *Pseudomonas aeruginosa* PAO1. *J Bacteriol*. 2003;185(3):1027–1036.
11. Kaplan JB, Ragunath C, Ramasubbu N, Fine DH. Detachment of *Actinobacillus actinomycetemcomitans* biofilm cells by an endogenous beta-hexosaminidase activity. *J Bacteriol*. 2003;185(16):4693–4698.
12. Lequette Y, Greenberg EP. Timing and localization of rhamnolipid synthesis gene expression in *Pseudomonas aeruginosa* biofilms. *J Bacteriol*. 2005; 187(1):37–44.
13. Nakano MM, Zuber P. Cloning and characterization of *srfB*, a regulatory gene involved in surfactin production and competence in *Bacillus subtilis*. *J Bacteriol*. 1989;171(10):5347–5353.
14. Mehlin C, Headley CM, Klebanoff SJ. An inflammatory polypeptide complex from *Staphylococcus epidermidis*: isolation and characterization. *J Exp Med*. 1999;189(6):907–918.
15. Yao Y, Sturdevant DE, Otto M. Genomewide analysis of gene expression in *Staphylococcus epidermidis* biofilms: insights into the pathophysiology of *S. epidermidis* biofilms and the role of phenol-soluble modulins in formation of biofilms. *J Infect Dis*. 2005;191(2):289–298.
16. Queck SY, et al. RNAIII-Independent Target Gene Control by the *agr* Quorum-Sensing System: Insight into the Evolution of Virulence Regulation in *Staphylococcus aureus*. *Mol Cell*. 2008;32(1):150–158.
17. Vuong C, Durr M, Carmody AB, Peschel A, Klebanoff SJ, Otto M. Regulated expression of pathogen-associated molecular pattern molecules in *Staphylococcus epidermidis*: quorum-sensing determines pro-inflammatory capacity and production of phenol-soluble modulins. *Cell Microbiol*. 2004;6(8):753–759.
18. Wang R, et al. Identification of novel cytolytic peptides as key virulence determinants for community-associated MRSA. *Nat Med*. 2007;13(12):1510–1514.
19. Gill SR, et al. Insights on evolution of virulence and resistance from the complete genome analysis of an early methicillin-resistant *Staphylococcus aureus* strain and a biofilm-producing methicillin-resistant *Staphylococcus epidermidis* strain. *J Bacteriol*. 2005;187(7):2426–2438.
20. Zhang YQ, et al. Genome-based analysis of virulence genes in a non-biofilm-forming *Staphylococcus epidermidis* strain (ATCC 12228). *Mol Microbiol*. 2003;49(6):1577–1593.
21. Mack D, Nedelmann M, Krokotsch A, Schwarzkopf A, Heesemann J, Laufs R. Characterization of transposon mutants of biofilm-producing *Staphylococcus epidermidis* impaired in the accumulative phase of biofilm production: genetic identification of a hexosamine-containing polysaccharide intercellular adhesin. *Infect Immun*. 1994;62(8):3244–3253.
22. Vuong C, Gotz F, Otto M. Construction and characterization of an agr deletion mutant of *Staphylococcus epidermidis*. *Infect Immun*. 2000;68(3):1048–1053.
23. Kong KF, Vuong C, Otto M. *Staphylococcus* quorum sensing in biofilm formation and infection. *Int J Med Microbiol*. 2006;296(2–3):133–139.
24. Rohde H, et al. Polysaccharide intercellular adhesin or protein factors in biofilm accumulation of *Staphylococcus epidermidis* and *Staphylococcus aureus* isolated from prosthetic hip and knee joint infections. *Biomaterials*. 2007;28(9):1711–1720.
25. Kogan G, Sadovskaya I, Chaignon P, Chokr A, Jabbouri S. Biofilms of clinical strains of *Staphylococcus* that do not contain polysaccharide intercellular adhesin. *FEMS Microbiol Lett*. 2006;255(1):11–16.
26. Vuong C, Kocianova S, Yao Y, Carmody AB, Otto M. Increased colonization of indwelling medical devices by quorum-sensing mutants of *Staphylococcus epidermidis* in vivo. *J Infect Dis*. 2004;190(8):1498–1505.
27. Vuong C, Kocianova S, Yu J, Kadurugamuwa JL, Otto M. Development of real-time in vivo imaging of device-related *Staphylococcus epidermidis* infection in mice and influence of animal immune status on susceptibility to infection. *J Infect Dis*. 2008; 198(2):258–261.
28. Boles BR, Horswill AR. Agr-mediated dispersal of *Staphylococcus aureus* biofilms. *PLoS Pathog*. 2008; 4(4):e1000052.
29. Yarwood JM, Bartels DJ, Volper EM, Greenberg EP. Quorum sensing in *Staphylococcus aureus* biofilms. *J Bacteriol*. 2004;186(6):1838–1850.
30. Vuong C, Gerke C, Somerville GA, Fischer ER, Otto M. Quorum-sensing control of biofilm factors in *Staphylococcus epidermidis*. *J Infect Dis*. 2003; 188(5):706–718.
31. Vuong C, Saenz HL, Gotz F, Otto M. Impact of the *agr* quorum-sensing system on adherence to polystyrene in *Staphylococcus aureus*. *J Infect Dis*. 2000; 182(6):1688–1693.
32. Ji G, Beavis R, Novick RP. Bacterial interference caused by autoinducing peptide variants. *Science*. 1997;276(5321):2027–2030.
33. Otto M. Quorum-sensing control in Staphylococci -- a target for antimicrobial drug therapy? *FEMS Microbiol Lett*. 2004;241(2):135–141.
34. Wright JS 3rd, Jin R, Novick RP. Transient interference with staphylococcal quorum sensing blocks abscess formation. *Proc Natl Acad Sci U S A*. 2005;102(5):1691–1696.
35. Chaignon P, Sadovskaya I, Ragunah C, Ramasubbu N, Kaplan JB, Jabbouri S. Susceptibility of staphylococcal biofilms to enzymatic treatments depends on their chemical composition. *Appl Microbiol Biotechnol*. 2007;75(1):125–132.
36. Otto M. Staphylococcal biofilms. *Curr Top Microbiol Immunol*. 2008;322:207–228.
37. Watson DC, Yaguchi M, Bisaillon JG, Beaudet R, Morosoli R. The amino acid sequence of a gonococcal growth inhibitor from *Staphylococcus haemolyticus*. *Biochem J*. 1988;252(1):87–93.
38. Donvito B, Etienne J, Denoroy L, Greenland T, Benito Y, Vandenesch F. Synergistic hemolytic activity of *Staphylococcus lugdunensis* is mediated by three peptides encoded by a non-*agr* genetic locus. *Infect Immun*. 1997;65(1):95–100.
39. Bruckner R. Gene replacement in Staphylococcus carnosus and Staphylococcus xylosus. *FEMS Microbiol Lett*. 1997;151(1):1–8.
40. Kocianova S, et al. Key role of poly-gamma-DL-glutamic acid in immune evasion and virulence of *Staphylococcus epidermidis*. *J Clin Invest*. 2005;115(3):688–694.
41. Seeber S, Kessler C, Gotz F. Cloning, expression and characterization of the Sau3AI restriction and modification genes in *Staphylococcus carnosus* TM300. *Gene*. 1990;94(1):37–43.
42. Gu J, et al. Bacterial insertion sequence IS256 as a potential molecular marker to discriminate invasive strains from commensal strains of *Staphylococcus epidermidis*. *J Hosp Infect*. 2005;61(4):342–348.
43. Galdbart JO, Allignet J, Tung HS, Ryden C, El Solh N. Screening for *Staphylococcus epidermidis* markers discriminating between skin-flora strains and those responsible for infections of joint prostheses. *J Infect Dis*. 2000;182(1):351–355.
44. Vuong C, et al. A crucial role for exopolysaccharide modification in bacterial biofilm formation, immune evasion, and virulence. *J Biol Chem*. 2004; 279(52):54881–54886.